Appl Biochem Biotechnol
https://doi.org/10.1007/s12010-018-2835-y

Half Sandwich Rhodium(III) and Iridium(III) Complexes as Cytotoxic and Metallonuclease Agents

Pankajkumar A. Vekariya[1] · **Parag S. Karia**[1] · **Bhupesh S. Bhatt**[1] · **Mohan N. Patel**[1]

Received: 21 April 2018 / Accepted: 2 July 2018

Abstract Half sandwich complexes of the type $[(\eta 5\text{-}C_5Me_5)M(L^{1-3})Cl]Cl.2H_2O$ were synthesized using $[\{(\eta^5\text{-}C_5Me_5)M(\mu\text{-}Cl)Cl\}_2]$, where M = Rh(III)/Ir(III) and L^{1-3} = pyrimidine-based ligands. The complexes were characterized by spectral analysis. DNA interaction studies by absorption titration and hydrodynamic measurement and suggest intercalative mode of binding of complexes with CT-DNA. The molecular docking study also supports intercalation of the complexes between the stacks of nucleotide base pairs. The gel electrophoresis assay demonstrated the ability of the complexes to interact and cleave plasmid DNA. Minimum inhibitory concentrations (MIC) of the complexes were investigated by the microdilution broth method. The cytotoxic properties of the metal complexes were evaluated using brine shrimp lethality bioassay.

Keywords Half sandwich compounds · Rh(III)/Ir(III) metal complexes · NMR · Molecular docking

Introduction

The discovery of chemical nuclease activity of transition metal complexes and exploring their application in antineoplastic medication, molecular biology, and bioengineering have become hotspots in recent years [1, 2]. Transition metal complexes offer enormous scope for the design of anticancer candidates due to the large diversity of structure, bonding modes, and the wide

Electronic supplementary material The online version of this article (https://doi.org/10.1007/s12010-018-2835-y) contains supplementary material, which is available to authorized users.

✉ Mohan N. Patel
jeenen@gmail.com

Bhupesh S. Bhatt
bhupeshbhatt31@gmail.com

[1] Department of Chemistry, Sardar Patel University, Vallabh Vidyanagar, Gujarat 388120, India

Published online: 13 July 2018

range of ligand substitution rates [3]. The anticancer activity of most of the transition metal complexes is mainly due to the formation of metal-DNA adducts which interfere DNA replication and results in cell death [4].

After discovery as an antitumor agent, cisplatin represents today one of the most successful metal-based drugs in chemotherapy. The undesirable side effects and easily acquired drug resistance of platinum-based drugs stimulated tremendous research efforts in the field of medicinal inorganic chemistry [5, 6]. It is expected that transition metal-based anticancer drugs with mechanisms of action different from those of the platinum-based drugs would demonstrate diminished side effects, less tendency to acquire drug resistance and the broader spectrum of anticancer activities [7, 8]. Recently transition metal complexes received significant attention for their anticancer activity [7, 9–19].

Pyrimidine-based scaffolds have been explored for diverse biological applications in a recent decade [20–22], but the literature lacks more information about their DNA interaction and anticancer activities. So, exploring the application of pyrimidine-based metal complexes could bring a major breakthrough in medicinal inorganic chemistry, and within this context, herein, we report synthesis, characterization, and biological activities of half sandwich Rh(III) and Ir(III) complexes with pyrimidine-based neutral bidentate ligand.

Experimental Section

Materials and Reagents

All the chemicals were of analytical grade. Solvents were dried and distilled prior to their use by following standard procedure [23]. Dinuclear dichloro complexes [$\{(\eta^5\text{-}C_5Me_5)M(\mu\text{-}Cl)Cl\}_2$] (M = Rh/Ir) were prepared (Supply. 1) according to the literature method [24–26]. $RhCl_3.2H_2O$, $IrCl_3.2H_2O$, CT-DNA, bromophenol blue, acetic acid, and ethylenediaminetetraacetic acid disodium salt (EDTA) were purchased from S. D. Fine-Chem Limited, Mumbai, India. Agarose, Luria broth, ethidium bromide, and Tris(hydroxymethyl)methylamine (Tris-HCl) were purchased from Hi-media Laboratories Pvt. Ltd., India. Culture of pUC19 (MTCC 47), two Gram$^{(+ve)}$ i.e., *Staphylococcus aureus* (*S. aureus*) (MTCC–3160), *Bacillus subtilis* (*B. subtilis*) (MTCC–7193) and three Gram$^{(-ve)}$ i.e., *Serratia marcescens* (*S. marcescens*) (MTCC–7103), *Pseudomonas aeruginosa* (*P. aeruginosa*) (MTCC–1688), and *Escherichia coli* (*E. coli*) (MTCC–433) bacterial species were purchased from the Institute of Microbial Technology (Chandigarh, India).

Physical Measurements

Euro Vector EA3000 elemental analyzer (240) was used to analyze carbon, hydrogen, and nitrogen content of the compounds. Thermogravimetric analysis and differential scanning calorimetric study were performed with a model 5000/2960 SDTA, TA instrument (USA). The ^{1}H NMR spectra were recorded on a Bruker Avance (400 MHz). Infrared spectra were recorded on an FT-IR Shimadzu spectrophotometer as KBr pellets in the range 4000 to 400 cm^{-1}. In the range 800 to 200 nm, the absorption spectra of the complexes were recorded on UV-160A UV–vis spectrophotometer, Shimadzu, Japan and 10-mm path length quartz cell. The magnetic moments were measured by Gouy's method using mercury tetrathiocyanatocobaltate(II) as the calibrant ($\chi_g = 16.44 \times 10^{-6}$ cgs units at 20 °C). The

diamagnetic correction was made using Pascal's constant. Photo quantization of the gel after electrophoresis was carried out on AlphaDigiDocTM RT, Version V.4.0.0 PC–Image software.

Synthesis

The reaction of 2-acetyl pyridine with different substituted aldehydes in 10% aq. NaOH and 30 ml methanol was carried out to yield corresponding chalcones. To a solution of guanidine hydrochloride (1.5 equiv.) in 50 mL of absolute ethanol, potassium t-butoxide (1.1 equiv.) was added. The reaction mixture was refluxed for 15 min and then the solution of chalcone (1.0 equiv.) in methanol was added to it and further refluxed for 6 h to afford the corresponding pyrimidine derivatives, i.e., ligands L^n (Supply. 2). The progress of the reaction was measured by TLC (40% Ethyl acetate/Hexane). The solvent was removed from the reaction mixture under reduced pressure. Water was added and the aqueous phase was extracted with chloroform (3 × 20 mL). The organic phases were dried over anhydrous Na_2SO_4, filtered, and concentrated. The crude product was purified by crystallization from ethanol or sometimes by column chromatography (2% Methanol in chloroform) to afford the pure compounds. All the synthesized compounds were well characterized by spectroscopic methods such as LCMS, NMR, FT-IR, and elemental analysis.

4-(4-Fluorophenyl)-6-(pyridin-2-yl)pyrimidin-2-amine (L^1)

Mp: 131–133 °C. Yield: 58%. FT-IR (KBr, 4000–400 cm^{-1}): 3340 ν(NH_2); 3059, 3003 ν(C–H)ar; 1537, 1477 ν(C = C); 1361 ν(C = N); 1230 ν(C–F); 1361 (pyridine skeleton band); 840 δ(C–H). ^{1}H NMR ($CDCl_3$, 400 MHz) *δ*/ppm: 8.775–8.703 (4H, m, phenyl), 8.581 (1H, dd, *J* = 2.0, 8.4 Hz, pyridyl), 8.145 (1H, s, pyrimidyl), 7.917 (1H, dd, *J* = 8.0, 8.8 Hz, pyridyl), 7.259 (1H, dd, *J* = 7.6 Hz, pyridyl), 7.076 (1H, dd, *J* = 2.8, 8.4 Hz, pyridyl), 6.645 (2H, s, amine). ^{13}C NMR ($CDCl_3$, 100 MHz) *δ*/ppm: 163.61 (C), 158.93 (C), 155.76 (C), 154.56 (C), 153.60 (C), 148.27 (CH), 139.45 (CH), 132.58 (CH), 130.23 (C), 123.43 (CH), 121.46 (CH), 113.64 (CH), 104.34 (CH). Anal. Calcd. for $C_{15}H_{11}FN_4$: C, 67.66; H, 4.16; N, 21.04. Found: C, 67.64; H 4.15; N 21.06.

4-(4-Chlorophenyl)-6-(pyridin-2-yl)pyrimidin-2-amine (L^2)

Mp: 154–156 °C. Yield: 69%. FT-IR (KBr, 4000–400 cm^{-1}): 3325 ν(NH_2); 3055, 3001 ν(C–H)ar; 1535, 1473 ν(C = C); 1392 ν(C = N); 1091 ν(C–Cl); 1357 (pyridine skeleton band); 829 δ(C–H). ^{1}H NMR ($CDCl_3$, 400 MHz) *δ*/ppm: 8.824 (2H, dd, *J* = 2.4, 8.8 Hz, phenyl), 8.702 (2H, dd, *J* = 2.4, 8.8 Hz, phenyl), 8.512 (1H, dd, *J* = 2.4, 7.2 Hz, pyridyl), 8.378 (1H, s, pyrimidyl), 8.092 (1H, dd, *J* = 8.0 Hz, pyridyl), 7.774 (1H, dd, *J* = 7.6 Hz, pyridyl), 7.340 (1H, dd, *J* = 2.4, 8 Hz, pyridyl), 6.639 (2H, s, amine). ^{13}C NMR ($CDCl_3$, 100 MHz) *δ*/ppm: 160.52 (C), 155.37 (C), 154.64 (C), 153.43 (C), 149.77 (CH), 142.68 (C), 138.31 (CH), 132.24 (C), 127.82 (CH), 124.65 (CH), 123.15 (CH), 121.47 (CH), 104.55 (CH). Anal. Calcd. for $C_{15}H_{11}ClN_4$: C, 63.72; H, 3.92; N, 19.82. Found: C, 63.70; H, 3.95; N, 19.80.

4-(4-Bromophenyl)-6-(pyridin-2-yl)pyrimidin-2-amine (L^3)

Mp: 140–142 °C. Yield: 67%. FT-IR (KBr, 4000–400 Cm^{-1}): 3325 ν(NH_2); 3055, 3005 ν(C–H)Ar; 1539, 1485 ν(C = C); 1361 ν(C = N); 1157, 825 (*p*–Substituted Aromatic Ring); 1009

ν(C–Br); 786 ν(C–H). ^{1}H NMR ($CDCl_3$, 400 MHz) δ/Ppm: 8.752 (2H, Dd, J = 2.4, 7.6 Hz, Phenyl), 8.701 (1H, S, Pyrimidyl), 8.510 (2H, Dd, J = 2.4, 8 Hz, Phenyl), 8.364 (1H, Dd, J = 2.4, 6.8 Hz, Pyridyl), 7.994 (1H, Dd, J = 8 Hz, Pyridyl), 7.623 (1H, Dd, J = 7.2 Hz, Pyridyl), 7.323 (1H, dd, J = 2.4, 8 Hz, Pyridyl), 6.651 (2H, S, Amine). ^{13}C NMR ($CDCl_3$, 100 MHz) δ/Ppm: 160.71 (C), 158.12 (C), 155.73 (C), 153.83 (C), 150.12 (CH), 137.37 (CH), 133.19 (CH), 131.05 (CH), 130.03 (C), 124.79 (CH), 123.87 (CH), 123.11 (C), 105.24 (CH). Anal. Calcd. For $C_{15}H_{11}BrN_4$: C, 55.06; H, 3.39; N, 17.12. Found: C, 55.08; H, 3.32; N, 17.15.

Synthesis of Complexes

To a solution of the dinuclear dichloro complex [{(η^5-C_5Me_5)M(μ-Cl)Cl}$_2$] (0.20 mmol) in CH_2Cl_2 (10 mL), an excess of the solid ligand (L^1-L^3) was added. The resulting mixture was stirred at room temperature for 16 h. Then the solution was filtered through Celite in order to remove solid particles, and the solvent was removed under reduced pressure. The residue was dissolved in methanol (5 mL), and the product was precipitated by addition of diethyl ether (30 mL), isolated by filtration, and dried in vacuo to obtain the corresponding complexes (Scheme 1). The complexes are soluble in methanol, ethanol, acetone, dichloromethane, chloroform, acetonitrile, dimethylformamide, and dimethyl sulphoxide but insoluble in petroleum ether and diethyl ether. The metal complexes were characterized by various analytical and spectroscopic methods. The ^{1}H-NMR, ^{13}C-NMR, and IR spectra of metal complexes were provided in the supplementary material (Supply. 3).

[(η^5-C_5Me_5)Rh(L^1)Cl]Cl·2H^2O (1)

Mp: 221–223 °C. Yield: 89%. FT-IR (KBr, 4000–340 cm^{-1}): 347 ν(Rh–Cl); 779 δ(C–H); 1026, 848 (*p*–substituted aromatic ring); 1381, 1234 (pyridine skeleton band); 1481 ν(C=N); 1589 ν(C=Npyridyl); 1658 ν(C=C); 3070 ν(C–H)ar; 3441 ν(N-H). ^{1}H NMR (DMSO, 400 MHz) δ/ppm: 8.801–8.723 (4H, m, phenyl), 8.624 (1H, dd, J = 2.0, 8.4 Hz, pyridyl), 8.423 (1H, s, pyrimidyl), 8.020–7.978 (1H, ddpoor resolved, pyridyl), 7.417–7.378 (1H, ddpoor resolved, pyridyl), 7.235 (1H, dd, J = 2.8, 8.4 Hz, pyridyl), 6.678 (2H, s, amine), 1.597 (15H, s, Cp). ^{13}C NMR (DMSO, 100 MHz) δ/ppm: 169.92 (C), 163.76 (d, J = 275 Hz, C), 162.08 (C), 158.12 (C), 149.16 (CH), 135.00 (CH), 134.68 (CH), 130.80 (C), 128.81 (CH), 128.48 (CH), 126.30 (C), 114.94 (CH), 112.19 (CH), 94.74 (Cp), 8.36 (Cp). Anal. Calcd. for $C_{25}H_{30}Cl_2FN_4O_2Rh$: C, 49.12; H, 4.95; N, 9.16; Rh, 16.83. Found: C, 49.56; H, 4.65; N, 9.35; Rh, 16.95.

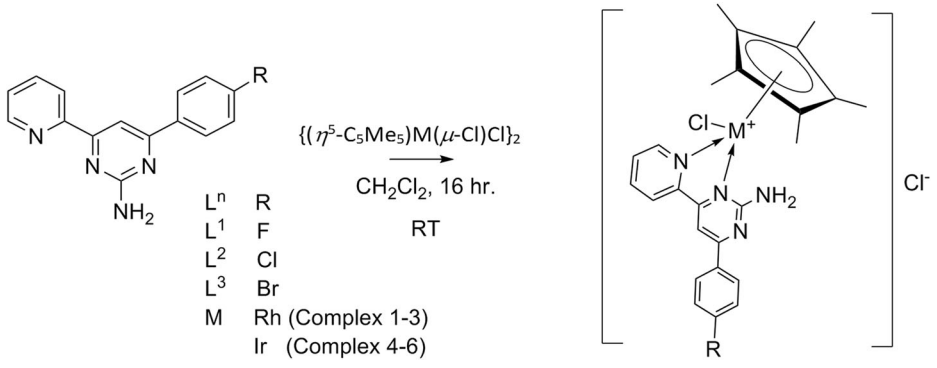

Scheme 1 Reaction scheme for the synthesis of complexes 1–6

[(η^5-C_5Me_5)Rh(L^2)Cl]Cl·2H_2O (2)

Mp: 203–205 °C. Yield: 95%. FT-IR (KBr, 4000–340 cm^{-1}): 378 ν(Rh–Cl); 779 δ(C–H); 1087, 840 (*p*–substituted aromatic ring); 1381, 1242 (pyridine skeleton band); 1473 ν(C=N); 1589 ν(C=Npyridyl); 1692 ν(C=C); 3070 ν(C–H)ar; 3443 ν(N-H). ^{1}H NMR (DMSO, 400 MHz) *δ*/ppm: 8.860–8.742 (4H, m, phenyl) 8.590 (1H, dd, $J = 2.4$, 7.2 Hz, pyridyl), 8.456 (1H, s, pyrimidyl), 8.167–8.126 (1H, ddpoor resolved, pyridyl), 7.851–7.814 (1H, ddpoor resolved, pyridyl), 7.422 (1H, dd, $J = 2.4$, 8 Hz, pyridyl), 6.675 (2H, s, amine), 1.596 (15H, s, Cp). ^{13}C NMR (DMSO, 100 MHz) *δ*/ppm: 170.02 (C), 162.80 (C), 157.88 (C), 149.36 (CH), 142.65 (C), 134.94 (CH), 133.86 (CH), 131.85 (C), 129.34 CH), 124.51 (C), 123.33 (CH), 119.08 (CH), 115.88 (CH), 94.58 (Cp), 8.63 (Cp). Anal. Calcd. for $C_{25}H_{30}Cl_3N_4O_2Rh$: C, 47.83; H, 4.82; N, 8.92; Rh, 16.39. Found: C, 47.55; H, 4.62; N, 8.75; Rh, 16.58.

[(η^5-C_5Me_5)Rh(L^3)Cl]Cl·2H_2O (3)

Mp: 227–229 °C. Yield: 90%. FT–IR (KBr, cm–1): 357 ν(Rh–Cl); 786 δ(C–H); 1010, 835 (*p*–substituted aromatic ring); 1357, 1288 (pyridine skeleton band); 1481 ν(C=N); 1543, ν(C=Npyridyl); 1674 ν(C=C); 3062 ν(C–H)ar; 3434 ν(N-H). ^{1}H NMR (DMSO, 400 MHz) *δ*/ppm: 8.812–8.764 (4H, m, phenyl), 8.576 (1H, dd, $J = 2.4$, 7.2 Hz, pyridyl), 8.432 (1H, s, pyrimidyl), 8.207–8.167 (1H, ddpoor resolved, pyridyl), 7.731–7.695 (1H, ddpoor resolved, pyridyl), 7.432 (1H, dd, $J = 2.4$, 8 Hz, pyridyl), 6.677 (2H, s, amine), 1.610 (15H, s, Cp). ^{13}C NMR (DMSO, 100 MHz) *δ*/ppm: 169.66 (C), 163.14 (C), 160.31 (C), 151.34 (CH), 135.16 (CH), 133.24 (CH), 130.14 (C), 129.69 (CH), 129.05 (CH), 127.44 (CH), 125.55 (C), 122.70 (C), 115.18 (CH), 94.08 (Cp), 8.69 (Cp). Anal. Calcd. for $C_{25}H_{30}BrCl_2N_4O_2Rh$: C, 44.67; H, 4.50; N, 8.33; Rh, 15.31. Found: C, 44.13; H, 4.22; N, 8.19; Rh, 15.61.

[(η^5-C_5Me_5)Ir(L^1)Cl]Cl·2H_2O (4)

Mp: 242–244 °C. Yield: 96%. FT-IR (KBr, 4000–340 cm^{-1}): 354 ν(Ir–Cl); 779 δ(C–H); 1034, 848 (*p*–substituted aromatic ring); 1381, 1234 (pyridine skeleton band); 1481 ν(C=N); 1540 ν(C=Npyridyl); 1597 ν(C=C); 3070 ν(C–H)ar; 3427 ν(N-H). ^{1}H NMR (DMSO, 400 MHz) *δ*/ppm: 8.808–8.734 (4H, m, phenyl), 8.692 (1H, dd, $J = 2.0$, 8.0 Hz, pyridyl), 8.486 (1H, s, pyrimidyl), 8.194–8.153 (1H, ddpoor resolved, pyridyl), 7.496–7.456 (1H, ddpoor resolved, pyridyl), 7.327 (1H, dd, $J = 2.8$, 8.4 Hz, pyridyl), 6.685 (2H, s, amine), 1.621 (15H, s, Cp). ^{13}C NMR (DMSO, 100 MHz) *δ*/ppm: 170.80 (C), 164.81 (C), 162.77 (C), 158.58 (C), 150.20 (CH), 136.17 (CH), 134.97 (CH), 132.12 (C), 128.62 (CH), 127.47 (CH), 126.51 (C), 116.59 (CH), 113.89 (CH), 95.69 (Cp), 9.11 (Cp). Anal. Calcd. for $C_{25}H_{30}Cl_2FIrN_4O_2$: C, 42.86; H, 4.32; Ir, 27.43; N, 8.00. Found: C, 42.17; H, 4.52; Ir, 27.46; N, 8.15.

[(η^5-C_5Me_5)Ir(L^2)Cl]Cl·2H_2O (5)

Mp: 213–215 °C. Yield: 95%. FT-IR (KBr, 4000–340 cm^{-1}): 351 ν(Ir –Cl); 779 δ(C–H); 1033, 840 (*p*–substituted aromatic ring); 1381, 1242 (pyridine skeleton band); 1481 ν(C=N); 1533 ν(C=Npyridyl); 1597 ν(C=C); 3062 ν(C–H)ar; 3421 ν(N-H). ^{1}H NMR (DMSO, 400 MHz) *δ*/ppm: 8.877–8.757 (4H, m, phenyl), 8.596 (1H, dd, $J = 2.4$, 7.2 Hz, pyridyl), 8.481 (1H, s, pyrimidyl), 8.241–8.200 (1H, ddpoor resolved, pyridyl), 7.925–7.887 (1H, ddpoor resolved, pyridyl), 7.437 (1H, dd, $J = 2.4$, 8.0 Hz, pyridyl), 6.681 (2H, s, amine), 1.631 (15H, s, Cp). ^{13}C NMR (DMSO, 100 MHz) *δ*/ppm: 173.09 (C), 163.83 (C), 158.04 (C), 150.24 (CH), 143.19 (C), 135.66 (CH), 134.24 (CH), 132.44 (C), 130.09 CH), 125.25 (C), 124.25 (CH), 119.62 (CH), 116.09 (CH), 95.32 (Cp), 9.79 (Cp). Anal. Calcd. for $C_{25}H_{30}Cl_3IrN_4O_2$: C, 41.87; H, 4.22; Ir, 26.80; N, 7.81. Found: C, 41.77; H, 4.17; Ir, 26.74; N, 7.75.

[(η^5-C_5Me_5)Ir(L^3)Cl]Cl·2H_2O (6)

Mp: 219–221 °C. Yield: 92%. FT-IR (KBr, 4000–340 cm–1): 362 ν(Ir–Cl); 771 δ(C–H); 1030, 833 (*p*–substituted aromatic ring); 1381, 1242 (pyridine skeleton band); 1481 ν(C=N); 1589 ν(C=Npyridyl); 1627 ν(C=C); 3078 ν(C–H)ar; 3417 ν(N-H). ^{1}H NMR (DMSO, 400 MHz) *δ*/ppm: 8.837–8.798 (4H, m, phenyl), 8.589 (1H, dd, $J = 2.8$, 7.6 Hz, pyridyl), 8.485 (1H, s, pyrimidyl), 8.254–8.214 (1H, ddpoor resolved, pyridyl), 7.797–7.758 (1H, ddpoor resolved, pyridyl), 7.482 (1H, dd, $J = 2.0$, 8.0 Hz, pyridyl), 6.682 (2H, s, amine), 1.652 (15H, s, Cp). ^{13}C NMR (DMSO, 100 MHz) *δ*/ppm: 170.37 (C), 164.79 (C), 161.57 (C), 152.01 (CH), 135.42 (CH), 134.20 (CH), 131.51 (C), 130.34 (CH), 129.49 (CH), 128.73 (CH), 126.54 (C), 123.24 (C), 116.16 (CH), 95.29 (Cp), 9.27 (Cp). Anal. Calcd. for $C_{25}H_{30}BrCl_2IrN_4O_2$: C, 39.43; H, 3.97; Ir, 25.24; N, 7.36. Found: C, 39.34; H, 3.88; Ir, 25.63; N, 7.30.

Antibacterial Activity

To understand quantitatively the magnitude of the antibacterial activity, minimum inhibitory concentrations (MIC) of ligands and metal complexes were investigated according to the literature [27, 28].

DNA Binding Studies

UV-Visible Absorption

The binding constants of the metal complexes to CT-DNA determined by optical titrations at room temperature were measured with 5 μM metal complex, and the CT-DNA concentration was varied from 0 to 100 μM (5 mM Tris/HCl, pH 7.5) as reported in the literature [29–31].

Viscosity Measurement

Viscosity measurement was performed in the thermostatic viscosity bath maintained at 37 ± 0.1 °C using Ubbelohde viscometer by measuring the flow time of DNA in Tris-HCl buffer, pH 7.2 as per the reported procedure [32–34].

Molecular Docking Study

The rigid molecular docking studies on complexes 1–6 have been performed using HEX 8.0 software. The crystal structure of the B-DNA dodecamer d(CGCGAATTCGCG)$_2$ was downloaded from the Protein Data Bank (PDB ID: 1BNA) (http://www.rcsb.org/pdb). The default parameters were used for docking calculation with correlation type shape only, FFT mode at 3D level, grid dimension of 6 with receptor range 180, and ligand range 180 with twist range 360 and distance range 40 [35, 36].

Chemical Nuclease Activity

For gel electrophoresis, 15 μL reaction mixture containing plasmid DNA in TE buffer (10 mM Tris, 1 mM EDTA, pH 8.0) and 200 μM complex were incubated for 24 h at 37 °C; followed by addition of 5 μL loading buffer (0.25% bromophenol blue, 40% sucrose, 0.25% xylene cyanole, and 200 mM EDTA) for reaction quenching. The gel was stained with 0.5 μg/mL EtBr and was

photographed on a UV illuminator. The percentage of each form of DNA was quantified using AlphaDigiDoc™ RT. Version V.4.0.0 PC–Image software. The degree of DNA cleavage activity was expressed in terms of the percent of cleavage of the SC-DNA according to the following Eq. 1:

$$\%\text{DNA cleavage activity} = \left[\frac{(\%\text{of SC}-\text{DNA})_{\text{control}} - (\%\text{of SC}-\text{DNA})_{\text{sample}}}{(\%\text{of SC}-\text{DNA})_{\text{control}}}\right] \times 100$$

Brine Shrimp Lethality Bioassay

The cytotoxicity of complexes was studied on brine shrimp, Artemia cysts, according to the method reported by Meyer et al. [37] for the series of complex concentrations, in vials containing 1450 μL sea salt solution + 1000 μL sea salt containing ten nauplii + 50 μL complex in 2% (*V*/*V*) DMSO. After 24 h of incubation, live and dead larvae were counted and LC_{50} was determined for each complex.

Result and Discussion

Analytical and Spectral Characterization

The molar conductivities of half sandwich Rh/Ir complexes in DMSO (10^{-3} M) at room temperature are observed in the range 81–96 Ω^{-1} cm^2 mol^{-1}, indicate the 1:1 electrolytic nature of the complexes [38]. The magnetic moment values of synthesized complexes are found to be zero, which indicates the absence of unpaired electron and diamagnetic nature of complexes. The TGA curve of complexes shows weight loss up to 120 °C, indicates the presence of two water molecules in the compounds as the water of crystallization [39]. The weight loss occurs from 320 to 600 °C corresponds to the loss of ligands and leaving behind the metal residue (Supply. 4).

The IR spectra of half sandwich complexes exhibit intense bands due to $\upsilon(C=N_{pyridyl})$ at 1533–1589 cm^{-1}, in conjunction with other bands associated with dipyridyl moieties. The IR spectral data support the coordination of the dipyridyl ligand and formation of the respective complexes. The band in complexes at 3417–3443 cm^{-1} is attributed to the υ(N-H) stretching vibration. The band around 3070 cm^{-1} are assigned to the υ(C-H)ar stretching of the ligands. ^{1}H-NMR and ^{13}C-NMR spectra of complexes indicate that the coordination of ligand results in shifting of all peaks of heterocyclic ring in the downfield region. This suggests that coordination occurs through N atom of pyrimidine and pyridine ring. The pentamethylcyclopentadienyl ligand gives rise to a characteristic singlet for all the methyl protons.

Antibacterial Activity

The in vitro antimicrobial activities of the complexes were screened against three Gram$^{(-ve)}$ bacteria, *Escherichia coli, Pseudomonas aeruginosa, Staphylococcus aureus*, and two Gram$^{(+ve)}$ bacteria, *Bacillus subtilis* and *Serratia marcescens*. The minimum inhibitory concentration values of complexes indicate that all the complexes are active against all the five different microorganisms compared to ligand and metal salt alone (Supply 5). The higher antimicrobial activity of the metal complexes (MIC = 180–369 μM) compared to the metal salt (MIC > 1000 μM) can be the result of chelate effects, nuclearity of the metal center in the complexes, nature of the ligands, and ion neutralizing the complexes [40].

DNA Binding Studies

UV-Visible Absorption

Electronic absorption spectroscopy is one of the most widely used techniques to follow the interaction of metal complexes with DNA. There are mainly two binding modes in the drug–DNA interaction, i.e., covalent binding and non-covalent binding mode (intercalative, electrostatic, and groove binding). Absorption titration study was performed to investigate the binding mode and intrinsic equilibrium binding constant (K_b) for the complexes with CT-DNA by monitoring the change in absorbance at various concentrations of DNA. DNA binding constants (K_b) was calculated from the Eq. 1 using the extinction coefficient of the compounds, the free complex concentration, and the ratio of bound complex per mole of DNA [41].

$$\frac{[\mathrm{DNA}]}{(\varepsilon_a - \varepsilon_f)} = \frac{[DNA]}{(\varepsilon_b - \varepsilon_f)} + \frac{1}{K_b(\varepsilon_b - \varepsilon_f)} \tag{1}$$

where, [DNA] = concentration of DNA in base pairs, ε_a = extinction coefficient observed for the MLCT absorption band at the given DNA concentration, ε_f = the extinction coefficient of the complex in solution, and ε_b = the extinction coefficient of the complex when fully bound to DNA. The plot of [DNA]/($\varepsilon_a - \varepsilon_f$) vs [DNA] gave a slope 1/ ($\varepsilon_a - \varepsilon_f$) and intercept 1/$K_b$($\varepsilon_a - \varepsilon_f$), respectively. The intrinsic binding constant (K_b) is the ratio of the slope to the intercept [42].

The pronounced decreases in absorbance with bathochromic shifts of ~ 2 nm for the MLCT maxima at a wavelength of around ~ 295 nm (Fig. 1) indicate that complex intercalates in between the base pairs of DNA, the π^* orbital of the intercalated ligand of the complex couples with π orbital of the base pairs of DNA, thus decreasing the π-π^* transition energy and resulting in bathochromism. The K_b values of the complexes 1–6 are 9.48×10^5, 7.17×10^5, 4.66×10^5, 7.50×10^5, 5.85×10^5, and 3.55×10^5 M^{-1}, respectively. The plot of [DNA]/($\varepsilon_a - \varepsilon_f$) vs. [DNA] of complexes 1–6 are shown in supplementary 6. These values are comparable to the classical intercalator ethidium bromide (7.16×10^5 M^{-1}) [43], and higher than some metal complexes reported in literature [44–47].

Viscosity Measurement

The binding behavior was further confirmed by viscosity measurements. A classical intercalative mode causes an increase in the DNA viscosity due to increasing of overall length of DNA [48]. The relative viscosity of the DNA solutions increased progressively with an increase in the concentrations of all the complexes (Supply 7), which suggests intercalation of the complexes between the stacks of DNA base pairs and thus this study supports the UV-Vis. absorption data. The intercalation of complexes into the DNA lengthens the DNA base stacks, which results in an increase in the viscosity of the DNA solution.

Molecular Docking Study

DNA-binding is the critical step for the study of metal-based drugs, illuminating the mechanisms involved in site-specific DNA recognition and designing new types of pharmaceutical molecules. The binding behavior of the synthesized compounds toward DNA was explored both

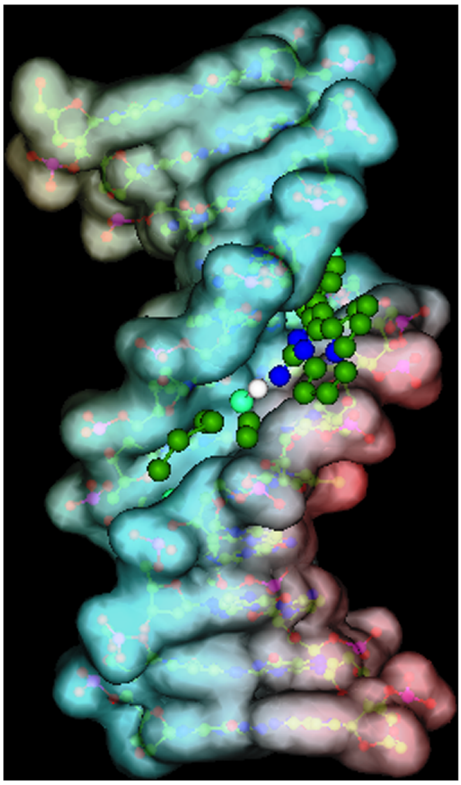

Fig. 1 Absorption spectra of complex 1 (5 μM) at 295 nm with increasing amount of CT DNA (0–60 μM) in Tris–HCl buffer (pH 7.2), with an incubation period of 10 min at room temperature. The arrow shows absorbance change with increasing DNA concentrations Inset: plot of [DNA]/ $(\varepsilon_a - \varepsilon_f)$ vs. [DNA]

theoretically and experimentally with the aid of different procedures and techniques. The theoretical evaluation includes the computational study of the interaction between compounds and DNA duplex with sequence $d(ACCGACGTCGGT)_2$. Docking was performed to preliminarily predict the binding affinity and binding site with the sterically acceptable conformations. Lower binding free energy implies a better binding interaction between the receptor (DNA) and "the ligand" molecules. The minimum energy docked pose clearly show minor groove with a rich G-C region as the first interaction site of metal complexes as shown in Fig. 2, followed by the intercalation of complexes in between the stacks of DNA base pairs as suggested by UV-Vis absorption study and viscosity measurement. The interaction is the result of van der Waals forces of attraction and hydrophobic contacts, and the binding energy or Docking scores obtained for the interaction of metal complexes 1–6 with DNA duplex sequence are − 322.09, − 323.86, − 323.86, − 321.90, − 324.64, and − 324.64 kJ mol^{-1}, respectively. The docked structure for complexes 1–6 are shown in supplementary 8. The negative values of the binding free energy of the docked complexes suggest reasonably binding of metal complexes with DNA.

Chemical Nuclease Activity

Gel electrophoresis experiment provides valuable information of plasmid DNA hydrolytic or oxidative cleavage reaction by compounds [49]. The cleaved DNA molecule migrates in the gel as a function of their mass, charge, and shape, with supercoiled DNA migrating faster than an open circular molecule of the same mass and charge [50]. The plasmid cleavage influenced

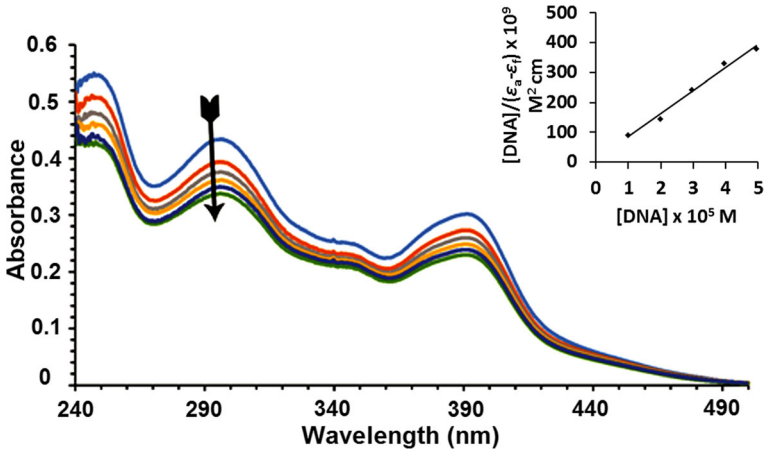

Fig. 2 Molecular docked model of complex 1 located within the hydrophobic pocket of DNA (PDB ID: 1BNA)

by metal salt and complexes is shown in Fig. 3, and data of plasmid cleavage is presented in Table 1. Here, all the complexes show the efficient cleavage ability (Supply 9). The similar DNA cleavage activity was shown by half sandwich Rh(III) and Ir(III) complexes in the literature [51]. The different DNA-cleavage efficiency of the complexes, metal salt, and drugs is due to the difference in binding affinity of the complexes to DNA and the structural dissimilarities of ligands [52]. This can be verified by the fact that complexes having larger binding constant value as evaluated by UV-Vis absorption study, are better nuclease agents. Also fluorine-containing ligands are better metallonuclease agents than ligands containing less electronegative Cl and bulkier Br atoms.

Brine Shrimp Lethality Bioassay

Brine shrimp lethality bioassay is a recent development in the assay procedure of bioactive compound, which indicates cytotoxicity as well as a wide range of pharmacological activities (such as anticancer, antiviral, insecticidal, and pesticidal) of the compounds. From the data (Table 1), the variation in lethality results may be due to the difference in the amount and kind of cytotoxic substances and substituents. The complexes show good cytotoxic activity against brine shrimps but this investigation is a primary one, and further tests are required to investigate its actual mechanism of cytotoxicity and its probable effects on cancer cell line

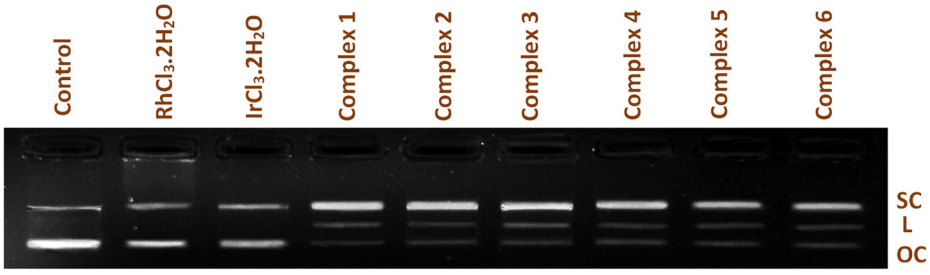

Fig. 3 Photogenic view of cleavage of pUC19 DNA with metal salts and a series of complexes 1–6 using 1% agarose gel containing 0.5 μM EB. All reactions were incubated in TE buffer (pH 8) at a final volume of 15 μL for 3 h at 37 °C

Table 1 Biological screening of the complexes

Complex	% Cleavage	LC_{50} (μg mL^{-1})
1	85.99	5.75
2	84.84	6.45
3	83.18	7.58
4	85.48	5.88
5	83.31	6.91
6	81.40	7.76

and higher animal model. It suggests that the complexes can be used as potent cytotoxic agents with the hope of adding an arsenal of weapons used against the fatal disease cancer.

Conclusions

Half sandwich metal complexes of pyrimidine-2-amine derivatives coordinated to Rh(III) and Ir(III) have been synthesized and characterized by various analytical and spectral techniques. NMR and FT-IR spectra suggest coordination of metal with N atom of pyridine and pyrimidine ring of ligands. Antimicrobial screening of the complexes shows that complexes are more potent antimicrobial agent than ligand and metal salt against all the microbes used for the study. Absorption titration, viscosity measurement and docking studies suggest that all complexes intercalate in between the stacks of DNA base pair. Such type of interaction is also supported by docking study. Gel electrophoresis of plasmid DNA in the presence of complexes evidenced metal complexes as potent chemical nucleases agents. From the above studies, complex 1 emerges as the most potent metallonuclease agent among all complexes, which can be attributed to its highest binding affinity with DNA. The highest nuclease activity and binding constant value of complex 1 may be attributed to its least bulky nature and having more electronegative F atom as a substituent ligand. The highest potency may be attributed to Brine shrimp lethality bioassay which proposes metal complexes as potent cytotoxic agents.

Acknowledgements We are thankful to the Head, Department of Chemistry, Sardar Patel University, India for making it convenient to work in a laboratory.

Funding Information This study was financially supported by the University Grant Commission for providing under the scheme “UGC-CAS” and BSR One Time Grant.

Compliance with Ethical Standards

Conflict of Interest The authors declare that they have no conflict of interest.

References

1. Gubendran, A., Kesavan, M. P., Ayyanaar, S., Mitu, L., Athappan, P., & Rajesh, J. (2017). Non-enolisable Knoevenagel condensate appended Schiff bases-metal (II) complexes: Spectral characteristics, DNA-binding and nuclease activities. *Spectrochimica Acta Part A: Molecular and Biomolecular Spectroscopy, 181*, 39–46.

2. Liu, J.-B., Yang, C., Ko, C.-N., Vellaisamy, K., Yang, B., Lee, M.-Y., Leung, C.-H., & Ma, D.-L. (2017). A long lifetime iridium(III) complex as a sensitive luminescent probe for bisulfite detection in living zebrafish. *Sensors and Actuators B: Chemical, 243*, 971–976.
3. Gasser, G., Ott, I., & Metzler-Nolte, N. (2011). Organometallic Anticancer Compounds. *Journal of Medicinal Chemistry, 54*(1), 3–25.
4. Johnstone, T. C., Suntharalingam, K., & Lippard, S. J. (2016). The next generation of platinum drugs: targeted Pt(II) agents, nanoparticle delivery, and Pt(IV) prodrugs. *Chemical Reviews, 116*(5), 3436–3486.
5. Muhammad, N., Sadia, N., Zhu, C., Luo, C., Guo, Z., & Wang, X. (2017). Biotin-tagged platinum(iv) complexes as targeted cytostatic agents against breast cancer cells. *Chemical Communications, 53*(72), 9971–9974.
6. Xu, G., Zhao, J., Gou, S., & Pang, J. (2015). Antitumor platinum(II) complexes of N-cyclobutyl-1R,2R-diaminocyclohexane with dicarboxylates as leaving groups. *Bioorganic & Medicinal Chemistry Letters, 25*(2), 221–224.
7. Leonidova, A., & Gasser, G. (2014). Underestimated potential of organometallic rhenium complexes as anticancer agents. *ACS Chemical Biology, 9*(10), 2180–2193.
8. Liu, Z., & Sadler, P. J. (2014). Organoiridium complexes: anticancer agents and catalysts. *Accounts of Chemical Research, 47*(4), 1174–1185.
9. Tian, M., Li, J., Zhang, S., Guo, L., He, X., Kong, D., Zhang, H., & Liu, Z. (2017). Half-sandwich ruthenium(ii) complexes containing N^N-chelated imino-pyridyl ligands that are selectively toxic to cancer cells. *Chemical Communications, 53*(95), 12810–12813.
10. Hegde, D., Dodamani, S., Kumbar, V., Jalalpure, S., & Gudasi, K. B. (2017). Synthesis, crystal structure, DNA interaction and anticancer evaluation of pyruvic acid derived hydrazone and its transition metal complexes. *Applied Organometallic Chemistry, 31*(12).
11. Wang, X. L., Zheng, K., Wang, L. Y., Li, Y. T., Wu, Z. Y., & Yan, C. W. (2016). Synthesis and structure of a new ternary monocopper(II) complex containing mixed ligands of 2,2′-diamino-4,4′-bithiazole and picrate: in vitroanticancer activity, molecular docking and reactivity towards DNA. *Applied Organometallic Chemistry, 30*(9), 730–739.
12. Nagaj, J., Kołkowska, P., Bykowska, A., Komarnicka, U. K., Kyzioł, A., & Jeżowska-Bojczuk, M. (2015). Interaction of methotrexate, an anticancer agent, with copper(II) ions: coordination pattern, DNA-cleaving properties and cytotoxic studies. *Medicinal Chemistry Research, 24*(1), 115–123.
13. Ahmadi, F., Saberkari, M., Abiri, R., Motlagh, H. M., & Saberkari, H. (2013). In vitro evaluation of Zn–Norfloxacin complex as a potent cytotoxic and antibacterial agent, proposed model for DNA binding. *Applied Biochemistry and Biotechnology, 170*(4), 988–1009.
14. Heydari, M., Moghadam, M. E., Tarlani, A., & Farhangian, H. (2017). DNA as a target for anticancer Phen-Imidazole Pd(II) complexes. *Applied Biochemistry and Biotechnology, 182*(1), 110–127.
15. Vellaisamy, K., Li, G., Ko, C.-N., Zhong, H.-J., Fatima, S., Kwan, H.-Y., Wong, C.-Y., Kwong, W.-J., Tan, W., & Leung, C.-H. (2018). Cell imaging of dopamine receptor using agonist labeling iridium(iii) complex. *Chemical Science, 9*(5), 1119–1125.
16. Wang, W., Vellaisamy, K., Li, G., Wu, C., Ko, C.-N., Leung, C.-H., & Ma, D.-L. (2017). Development of a long-lived luminescence probe for visualizing β-galactosidase in ovarian carcinoma cells. *Analytical Chemistry, 89*(21), 11679–11684.
17. Liu, L.-J., Wang, W., Huang, S.-Y., Hong, Y., Li, G., Lin, S., Tian, J., Cai, Z., Wang, H.-M. D., & Ma, D.-L. (2017). Inhibition of the Ras/Raf interaction and repression of renal cancer xenografts in vivo by an enantiomeric iridium(iii) metal-based compound. *Chemical Science, 8*(7), 4756–4763.
18. Pouryasin, Z., Yousefi, R., Nabavizadeh, S. M., Rashidi, M., Hamidizadeh, P., Alavianmehr, M.-M., & Moosavi-Movahedi, A. A. (2014). Anticancer and DNA binding activities of platinum (IV) complexes; importance of leaving group departure rate. *Applied Biochemistry and Biotechnology, 172*(5), 2604–2617.
19. Yousefi, R., Aghevlian, S., Mokhtari, F., Samouei, H., Rashidi, M., Nabavizadeh, S. M., Tavaf, Z., Pouryasin, Z., Niazi, A., & Faghihi, R. (2012). The anticancer activity and HSA binding Properties of the structurally related platinum (II) complexes. *Applied Biochemistry and Biotechnology, 167*(4), 861–872.
20. Saddik, A. A., El-Dean, K., Adel, M., El-Sokary, G. H., Hassan, K. M., Abbady, M. S., Ismail, I. A., & Saber, S. H. (2017). Synthesis and cytotoxicity of some Thieno[2,3-d]pyrimidine derivatives. *Journal of the Chinese Chemical Society, 64*(1), 87–93.
21. Gorle, S., Maddila, S., Chokkakula, S., Lavanya, P., Singh, M., & Jonnalagadda, S. B. (2016). Synthesis, biological activity of pyrimidine linked with morpholinophenyl derivatives. *Journal of Heterocyclic Chemistry, 53*(6), 1852–1858.
22. Mohana, K. N., Kumar, B. N. P., & Mallesha, L. (2013). Synthesis and biological activity of some pyrimidine derivatives. *Drug Invention Today, 5*(3), 216–222.
23. Furniss, B. S. H., J, A., Smith, P. W. G., & Tatchell, A. R. V. (2004). *Vogel's textbook of practical organic chemistry* (5th ed.). London: ELBS and Longman.

24. White, C., Yates, A., Maitlis, P., & Heinekey, D. (2007). (η5-Pentamethylcyclopentadienyl)Rhodium and Iridium Compounds *Inorganic Syntheses, 29*, 228–234.
25. Ball, R., Graham, W., Heinekey, D., Hoyano, J., McMaster, A., Mattson, B., & Michel, S. (1990). Synthesis and structure of dicarbonylbis(.eta.-pentamethylcyclopentadienyl)diiridium. *Inorganic Chemistry, 29*(10), 2023–2025.
26. Kang, J. W., Moseley, K., & Maitlis, P. M. (1969). Pentamethylcyclopentadienylrhodium and -iridium halides. I. Synthesis and properties. *Journal of the American Chemical Society, 91*(22), 5970–5977.
27. Fernandes, C., Horn Jr., A., Vieira-da-Motta, O., de Assis, V. M., Rocha, M. R., Mathias, L. d. S., Bull, É. S., Bortoluzzi, A. J., Guimarães, E. V., Almeida, J. C. A., & Russell, D. H. (2010). Synthesis, characterization and antibacterial activity of FeIII, CoII, CuII and ZnII complexes probed by transmission electron microscopy. *Journal of Inorganic Biochemistry, 104*(11), 1214–1223.
28. Patel, M., Chhasatia, M., & Bhatt, B. (2011). In vitro bacteriostatic and DNA interaction studies of drug-based mixed-ligand complexes of cobalt(II). *Medicinal Chemistry Research, 20*(2), 220–230.
29. Reichmann, M. E., Rice, S. A., Thomas, C. A., & Doty, P. (1954). A further examination of the molecular weight and size of desoxypentose nucleic acid. *Journal of the American Chemical Society, 76*(11), 3047–3053.
30. Patel, M. N., Bhatt, B. S., & Dosi, P. A. (2012). Thermal, spectral, and thermodynamic studies for evaluation of calf thymus DNA interaction activity of some copper(II) complexes. *Journal of Thermal Analysis and Calorimetry, 107*(1), 55–64.
31. Shahabadi, N., Kashanian, S., Shalmashi, K., & Roshanfekr, H. (2009). DNA Interaction with PtCl2(LL) (LL = Chelating Diamine Ligand: N,N-Dimethyltrimethylendiamine) Complex. *Applied Biochemistry and Biotechnology, 158*(1), 1–10.
32. Bi, S., Zhao, T., Wang, Y., Zhou, H., Pang, B., & Gu, T. (2015). *Spectrochimica Acta A, 150*, 921–927.
33. Patel, M. N., Dosi, P. A., & Bhatt, B. S. (2012). Synthesis, characterization and biological activities of ciprofloxacin drug based metal complexes. *Acta Chimica Slovenica, 59*, 622-631
34. Patel, M. N., Bhatt, B. S., & Dosi, P. A. (2012). Topoisomerase inhibition, nucleolytic and electrolytic contribution on DNA binding activity exerted by biological active analogue of coordination compounds. *Applied Biochemistry and Biotechnology, 166*(8), 1949–1968.
35. Arthi, P., Shobana, S., Srinivasan, P., Mitu, L., & Kalilur Rahiman, A. (2015). Synthesis, characterization, biological evaluation and docking studies of macrocyclic binuclear manganese(II) complexes containing 3, 5-dinitrobenzoyl pendant arms. *Spectrochimica Acta A, 143*, 49–58.
36. Mehta, J. V., Gajera, S. B., & Patel, M. N. (2016). Design, synthesis and biological evaluation of pyrazoline nucleus based homoleptic Ru(iii) compounds. *Medicinal Chemistry Communications, 7*(7), 1367–1380.
37. Meyer, B. N., Ferrigni, N. R., Putnam, J. E., Jacobsen, L. B., Nichols, D. E., & McLaughlin, J. L. (1982). Brine shrimp: a convenient general bioassay for active plant constituents. *Planta Medica, 45*(05), 31–34.
38. Rani, S., Kumar, S., & Chandra, S. (2011). Synthesis, structural, spectral, thermal and antimicrobial studies of palladium(II), platinum(II), ruthenium(III) and iridium(III) complexes derived from N,N,N,N-tetradentate macrocyclic ligand. *Spectrochimica Acta Part A: Molecular and Biomolecular Spectroscopy, 78*(5), 1507–1514.
39. Bellis, E., Hajba, L., Kovacs, B., Sandor, K., Kollar, L., & Kokotos, G. (2006). Three generations of α,γ-diaminobutyric acid modified poly(propyleneimine) dendrimers and their cisplatin-type platinum complexes. *Journal of Biochemical and Biophysical Methods, 69*(1-2), 151–161.
40. Dendrinou-Samara, C., Psomas, G., Raptopoulou, C. P., & Kessissoglou, D. P. (2001). Copper(II) complexes with phenoxyalkanoic acids and nitrogen donor heterocyclic ligands: structure and bioactivity. *Journal of Inorganic Biochemistry, 83*(1), 7–16.
41. Swavey, S., DeBeer, M., & Li, K. (2015). Photoinduced interactions of supramolecular Ruthenium(II) complexes with plasmid DNA: synthesis and spectroscopic, electrochemical, and DNA photocleavage studies. *Inorganic Chemistry, 54*(7), 3139–3147.
42. Asatkar, A. K., Tripathi, M., Panda, S., Pande, R., & Zade, S. S. (2017). Cu(I) complexes of bis(methyl)(thia/selena) salen ligands: synthesis, characterization, redox behavior and DNA binding studies. *Spectrochimica Acta Part A: Molecular and Biomolecular Spectroscopy, 171*, 18–24.
43. Singh, R., Jadeja, R. N., Thounaojam, M. C., Patel, T., Devkar, R. V., & Chakraborty, D. (2012). Synthesis, DNA binding and antiproliferative activity of ternary copper complexes of moxifloxacin and gatifloxacin against lung cancer cells. *Inorganic Chemistry Communications, 23*, 78–84.
44. Shahabadi, N., Hadidi, S., & Taherpour, A. A. (2014). Synthesis, characterization, and DNA binding studies of a new Pt(II) complex containing the drug Levetiracetam: combining experimental and computational methods. *Applied Biochemistry and Biotechnology, 172*(5), 2436–2454.
45. Dehkhodaei, M., Sahihi, M., Rudbari, H. A., Gharaghani, S., Azadbakht, R., Taheri, S., & Kajani, A. A. (2017). Studies of DNA- and HSA-binding properties of new nano-scale green synthesized Ni (II) complex

as anticancer agent using spectroscopic methods, viscosity measurement, molecular docking, MD simulation and QM/MM. *Journal of Molecular Liquids, 248*, 24–35.
46. Lo, K. K. W., Chung, C. K., & Zhu, N. (2006). Nucleic acid intercalators and avidin probes derived from luminescent cyclometalated iridium(III)-dipyridoquinoxaline and -dipyridophenazine complexes. *Chemistry-A European Journal, 12*(5), 1500–1512.
47. Lo, K. K.-W., & Tsang, K. H.-K. (2004). Bifunctional luminescent Rhenium(I) complexes containing an extended planar diimine ligand and a biotin moiety. *Organometallics, 23*(12), 3062–3070.
48. Shoair, A., El-Shobaky, A., & Azab, E. (2015). Synthesis, characterization, DNA binding and catalytic applications of Ru(III) complexes. *Spectrochimica Acta Part A: Molecular and Biomolecular Spectroscopy, 151*, 322–334.
49. Rabindra, G., & Mahyoub, M. (2010). London AiT & First5 Committee: the voice of London General Practice Trainees within the Royal College of General Practitioners (RCGP). *London Journal of Primary Care, 3*(1), 58–58.
50. Dhanaraj, C. J., & Johnson, J. (2016). Transition metal complexes of a novel quinoxaline-based tridentate ONO donor ligand: synthesis, spectral characterization, thermal,in vitropharmacological and molecular modeling studies. *Applied Organometallic Chemistry, 30*(10), 860–871.
51. Gras, M., Therrien, B., Süss-Fink, G., Casini, A., Edafe, F., & Dyson, P. J. (2010). Anticancer activity of new organo-ruthenium, rhodium and iridium complexes containing the 2-(pyridine-2-yl)thiazole N,N-chelating ligand. *Journal of Organometallic Chemistry, 695*(8), 1119–1125.
52. Liu, Y.-J., Guan, X.-Y., Wei, X.-Y., He, L.-X., Mei, W.-J., & Yao, J.-H. (2007). Ruthenium(II) complexes containing 2,9-dimethyl-1,10-phenanthroline and 4,4′-dimethyl-2,2′-bipyridine as ancillary ligands: synthesis, characterization and DNA-binding. *Transition Metal Chemistry, 33*, 289–294.